Climate change and water resources in the Bagmati River Basin, Nepal

Article *in* Theoretical and Applied Climatology · May 2013

DOI: 10.1007/s00704-013-0910-4

CITATIONS
66

READS
892

4 authors, including:

Mukand S Babel
Asian Institute of Technology
198 PUBLICATIONS **4,757** CITATIONS
SEE PROFILE

Anshul Agarwal
Regional Integrated Multi Hazard Early Warning Systems
13 PUBLICATIONS **287** CITATIONS
SEE PROFILE

Climate change and water resources in the Bagmati River Basin, Nepal

Mukand S. Babel, Shyam P. Bhusal, Shahriar M. Wahid & Anshul Agarwal

Theoretical and Applied Climatology

ISSN 0177-798X

Theor Appl Climatol
DOI 10.1007/s00704-013-0910-4

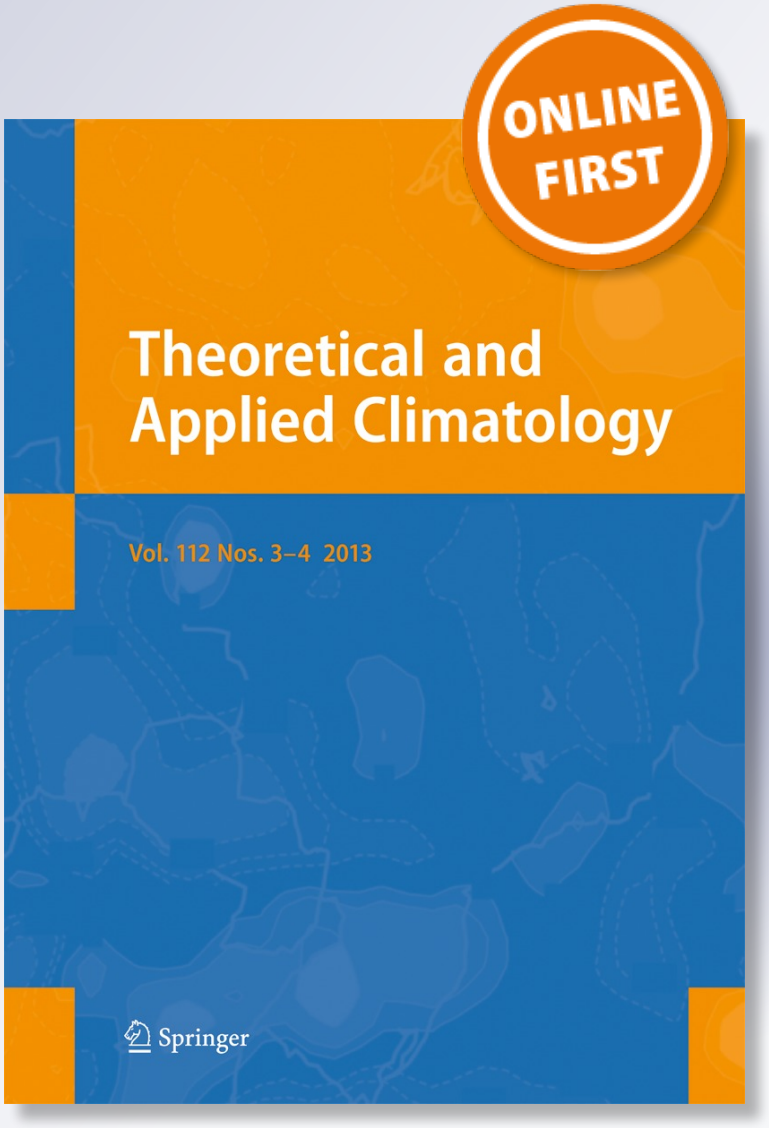

Springer

Theor Appl Climatol
DOI 10.1007/s00704-013-0910-4

ORIGINAL PAPER

Climate change and water resources in the Bagmati River Basin, Nepal

Mukand S. Babel · Shyam P. Bhusal · Shahriar M. Wahid · Anshul Agarwal

Received: 13 October 2012 / Accepted: 16 April 2013

Abstract This paper characterizes potential hydrological impact of future climate in the Bagmati River Basin, Nepal. For this research, basinwide future hydrology is simulated by using downscaled temperature and precipitation outputs from the Hadley Centre Coupled Model, version 3 (HadCM3), and the Hydrologic Engineering Center's Hydrologic Modeling System (HEC-HMS). It is predicted that temperature may rise maximally during the summer rather than winter for both A2 and B2 Special Report on Emissions Scenarios (SRES) scenarios. Precipitation may increase during the wet season, but it may decrease during other seasons for A2 scenario. For B2 scenario, precipitation may increase during all the seasons. Under the A2 scenario, premonsoon water availability may decrease more in the upper than the middle basin. During monsoons, both upper and middle basins show increased water availability. During the postmonsoon season, water availability may decrease in the upper part, while the middle part shows a mixed trend. Under the B2 scenario, water availability is expected to increase in the entire basin. The analysis of the projected hydrologic impact of climate change is expected to support informed decision-making for sustainable water management.

M. S. Babel (✉) · A. Agarwal
Water Engineering and Management, Asian Institute of Technology (AIT), PO Box 4 Klong Luang
Pathumthani 12120, Thailand
e-mail: msbabel@ait.asia

S. P. Bhusal
Hydroconsult Pvt. Ltd., Kathmandu, Nepal

S. M. Wahid
Integrated Water and Hazard Management Programme (IWHM), International Centre for Integrated Mountain Development (ICIMOD), Kathmandu, Nepal

1 Introduction

The Bagmati River Basin (BRB) is one of the major basins of Nepal and sustains much of the socioeconomic activities of the country. The basin's water is widely used for drinking, irrigation, industrial, and other purposes in the Kathmandu Valley, which comprises about 15 % of the basin area. Rivers in the basin possess rich cultural and heritage values (NTNC 2009). In recent time, increasing population density, unplanned rapid urbanization, land conversion to agriculture, and unregulated and illegal quarries have been responsible for degradation of the river water's quality and quantity (Babel et al. 2011). Sharma and Shakya (2006) studied seasonal variability and change in flood patterns for the period of 1965–2000 and found a decreasing trend in flood magnitude; however, duration and frequency of these floods are increasing.

It is postulated that changing hydrology of the BRB, fed by natural springs and monsoon precipitation (WECS 2011), can be attributed to climate change at different temporal and spatial scales. The Organization for Economic Cooperation and Development (OECD) (2003) used General Circulation Models (GCM) to show that in Nepal, the mean annual temperature is expected to increase by an average of 1.2 °C by 2030, 1.7 °C by 2050, and 3.0 °C by 2100 as compared to a pre-2000 baseline. The Institute for Social and Environmental Transition—Nepal (ISET-N 2009) used GCMs and Regional Circulation Models (RCM) and projected that the mean annual temperature in Nepal is expected to increase by 1.4 °C by 2030, 2.8 °C by 2060, and 4.7 °C by 2090. The models project almost no change in precipitation during winters (December to February) in western Nepal and up to a 5–10 % increase in precipitation in eastern Nepal. During the summer (June to September) the precipitation may increase by 15–20 % in the whole country towards the end of twenty-first century.

Published online: 22 May 2013

The change in frequency, timing, and amount of precipitation will affect river flow and occurrence of floods and droughts. The Third Assessment Report of the Intergovernmental Panel on Climate Change (IPCC 2001) reported the general impact of climate change on water resources and indicated an intensification of the global hydrological cycle affecting both ground and surface water supplies. Arnell (2003) and Nohara et al. (2006) used some of the most advanced global hydrological models, driven by ensembles of climate models, to understand the impact of climate change on river runoff. However, understanding the influence of climate change on the hydrological cycle on a global scale is inadequate for water resource planners at basin level due to their coarse (grid) resolution and the local heterogeneity of terrain and climate (Minville et al. 2008, IPCC 2001). A significant amount of effort has been expended in assessing the potential impact of climate change on basin water resources. Several studies have reported the impact of expected future climate on basin water resources (Hitz and Smith 2004, Christensen et al. 2004, Dore 2005, Harmsen et al. 2009, Chiew et al. 2009).

Yet, predicting the changing climate's impact on the hydrology of mountainous river basins is a complicated and uncertain process. The best interpolation of changes predicted by multiple GCMs provided by Arnell (2003) suggests corroborated increases in runoffs across the Himalayas, while changes in runoff from the Karakoram and Hindu-Kush ranges are highly model-dependant (Hadley Centre Coupled Model, version 3 (HadCM3) shows an increase of over 30 %, while the Commonwealth Scientific and Industrial Research Organization, Mark-2 model (CSIRO-MK2) shows a decrease of almost 20 % in the average annual runoff by 2050). Rees et al. (2004) developed a regional hydrological model for the Indus, Ganges, and Brahmaputra at a 20-km grid square resolution for a range of future climate scenarios to assess changes over the twenty-first century. Results from running the model with various hypothetical climate change scenarios for the entire Indus, Ganges, and Brahmaputra river basins suggest that water shortage is unlikely in many areas for at least several decades. In the Ganges, 5 % increase in mean annual runoff during 2070–2100 was predicted by Arora and Boer (2001). Jain (2008) finds it highly unlikely that the Ganges may become a seasonal river, particularly downstream of the Gangotri glacier.

Despite progress in understanding the impact of regional climate change on water resources and perceptible trends in the flow of the Himalayan Rivers, there has been a lack of comprehensive study to investigate the long-term effects of climate change on basin-scale water availability for the BRB. The uncertainty of future water availability on a basin scale has seriously impaired water resource planning in the BRB, thereby increasing the risk of failure of water-related programs and projects. To address the issue, this paper presents the analysis of future changes in local climate and their impact on the hydrology of the BRB to help in managing water more efficiently and making necessary plans of adaptation in changing climatic conditions.

2 Study area

The Bagmati River Basin is located within 26° 45′–27° 49′ north and 85° 02′–85° 57′ east, with a catchment area of about 3,750 km^2 in Nepal. The Bagmati River originates from the Shivapuri hills of the Mahabharat range, 25 km north of Kathmandu, the capital city of Nepal; passes through the inner Mahabharat range; stretches to the plain of Terai (the Nepal–India border); and reaches the River Ganges in India after traveling about 190 km through Nepal. The elevation in the basin varies from less than 80 m in the southern part to 2,900 m in the northern part of the basin.

The well-recognized four seasons in Nepal are winter (December to February), spring (March to May), summer (June to September), and autumn (October and November) (Shrestha et al., 1999). The climate of the BRB varies from cold temperate in higher mountains and warm temperate at mid-elevation levels to subtropical in the southern lowlands (<1,000 m msl) with a mean annual temperature of 20–30 °C. In the warm temperate climatic zone (1,000–2,000 m msl), the mean annual temperature range is 15–20 °C and in the cold temperate climatic zone (2,000–2,900 m msl), this value varies from 10 to 15 °C. The mean relative humidity varies from 70 to 86 %. The average annual rainfall in the basin is about 1,800 mm with 80 % of the total annual precipitation occurring during the summer. Snowfall is negligible in the basin. River flow is low during the spring and peaks during the summer with maximum value during July or August.

The BRB in Nepal is divided into three parts as upper (Kathmandu valley), middle (mountains/hills), and lower (Terai) considering the physiographic variation. This study, however, considers the upper (Kathmandu valley) and middle (mountains/hills) parts of the Bagmati Basin up to the Pandheradobhan gauging station, as shown in Fig. 1, with a total catchment area of 2,789 km^2. For the purpose of this research, the study area, therefore, consists of the upper and middle parts of the BRB. The upper part is covered by sub-basins 9 and 10 and the middle part includes sub-basins 11, 12, 13, 14, and 15 (Fig. 1).

The upper part of the basin comprises Kathmandu City. According to the 2001 census data, the total population in the basin was 2.3 million and about 69.5 % of the populace inhabits the upper basin. The higher population growth rate in the upper basin due to increasing migration of people to the capital city exerts a considerable challenge to water management in the basin. The climate change effect on future water availability may further exacerbate the situation.

Most of the catchment runoff of sub-basin 10 of the upper basin is diverted to East Rapti basin (not shown in Fig. 1). This diverted flow accounts for less than 3 % of the annual flow at the Pandheradobhan gauging station and expected to

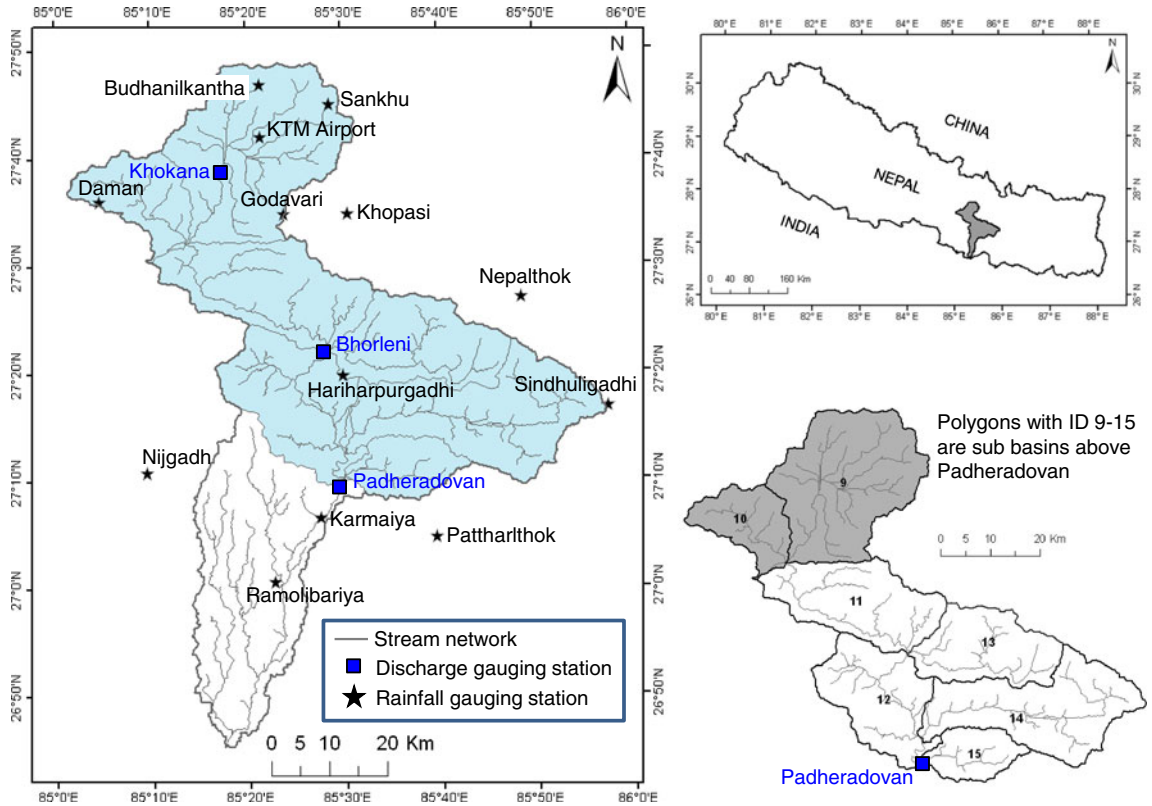

Fig. 1 The Bagmati River Basin

remain unchanged in the future. Hence, this diversion scheme was not considered in the analysis on climate change impact on hydrology.

3 Methodology

3.1 Data collection

3.1.1 GCM and NCEP reanalysis predictors

GCMs project global climatic variables under different emission scenarios but their resolution, representativeness of a particular area, and availability of data in the public domain necessitates conducting analysis prior to selecting a particular GCM for the BRB. In this study, a suit of five GCMs (CGCM3, CCSR, ECHAM4, HadCM3, and CSIRO-MK2) were analyzed to identify the most suitable GCM for the BRB. The performance of the five GCMs was evaluated based on three indicators: standard deviation (SD), coefficient of determination (R^2), and Root Mean Square Error (RMSE). All GCMs, except CSIRO-MK2, were found statistically reliable in reproducing present-day, observed-monthly, average precipitation. Four GCMs, i.e., HadCM3, CCSR, CGCM3, and ECHAM4, had considerably good R^2 values (varying from 0.10 to 0.68). However, HadCM3 had performed comparatively better with higher R^2 in most of the stations with values ranging from 0.38 to 0.6. Similarly, scenario B2 of HadCM3 model had SD close to SD of observed precipitation for most of the stations. HadCM3 B2 scenario also had considerably lower RMSE for most of the stations with its lowest value of 2.69 mm. Based on these results, HadCM3 was considered suitable for the study basin.

Large-scale predictor variables, commonly known as National Centers for Environmental Prediction (NCEP) reanalysis predictors, and HadCM3 predictors, corresponding to two Special Report on Emissions Scenarios (SRES) scenarios, A2 and B2, were downloaded from the Statistical Downscaling Model (SDSM) website, http://www.cics.uvic.ca/scenarios/sdsm/select.cgi. Since the NCEP reanalysis data is available normalized to the HadCM3 grid size, the predictors can be directly used as input files for the SDSM. The predictor files used are as follows:

NCEP_1961-2001: This file contains 41 years of daily observed predictor data derived from the NCEP reanalysis data.
H3A2a_1961-2099 and H3B2a_1961-2099: These files contain 139 years of daily GCM predictor data derived from HadCM3 A2 and B2 experiments, respectively.

3.1.2 Observed hydrometeorological data

Daily precipitation data for the period of 1970–2005 from nine stations in the basin was collected from the Department of Hydrology and Meteorology (DHM), Nepal (Table 1). Out of all the stations considered for the precipitation analysis using the Thiessen Polygon method, four stations (KTM Airport, Daman, Sankhu, and Godavary) contribute to the upper part of the BRB. Four other stations, Sindhuligadhi, Hariharpurgadhi, Ramolibariya, and Khopasi (although this station is physically located in the upper part), contribute to the middle basin (Fig. 1). Minimum and maximum temperature data were available only for the KTM Airport, Daman, Budhanilkantha, and Sindhuligadhi stations. The daily discharge data required for calibration and validation of the hydrological model was collected for the period of 1990–2006 from the Pandheradobhan gauging station that is also the outlet of the study area, and the upper and the middle parts of the BRB (Fig. 1).

3.1.3 Other data

The 90-m resolution Digital Elevation Model (DEM) was downloaded from the CGIAR-CSI website: http://srtm.csi.cgiar.org/SELECTION/inputCoord.asp. Land use and soil data for the year 1995 was obtained from the Bagmati Integrated Watershed Management Project and the Department of Soil Conservation and Watershed Management, Nepal. The major land use type in the BRB is agriculture and forest that cover about 35 and 57 %, respectively. The built-up area is about 0.74 %. Loamy soil is the most dominant in the basin.

3.2 Climate change scenario

3.2.1 Downscaling technique

GCMs are used to project long-term temperature and precipitation data. For the last 20 years, there have been significant improvements in the data quality of these models (Huntingford et al. 2006, Xu et al. 2008). Unfortunately, most GCMs provide data with a resolution of nearly 300 to 400 km, which is inadequate for basin-scale hydrological studies. This difference of resolutions between GCM data and basin-scale hydrological model input requirements necessitates downscaling of the GCM data. The general principle of downscaling is to relate large-scale predictor variables to subgrid- or station-level climate variables. In this study, the statistical downscaling method is used due to its simplicity and less computational time compared to dynamic downscaling (Prudhomme et al. 2002). Often, the dynamically downscaled data needs additional statistical downscaling, especially in mountainous regions like the BRB, where the climate varies spatially even at very short distances.

Many techniques are available for statistical downscaling. The SDSM version 4.2 (Wilby et al. 2002, Wilby and Dawson 2004, Wilby and Dawson 2007) was used for this study. It was widely used in the climate research field (Harpham and Wilby 2005, Dibike and Coulibaly 2005, Khan et al. 2006, Wilby et al. 2006, Xu et al. 2008, Toews and Allen 2009). This model uses the principle of developing multiple linear regression transfer function between large-scale predictors and local climatic variables (predictand) and these transfer functions are used for downscaling future climate data as predicted by GCMs. The principle of spatial downscaling is:

$$R = F(L)$$

where R represents the predictand (a local climatic variable), L represents predictors (a set of large scale climatic variables), and F represents the deterministic/stochastic relation conditioned by L.

Downscaling with SDSM consists of four major steps: (1) screening of large-scale climatic variables (predictors), (2) calibration of transfer functions, (3) validation of downscaling model results, and (4) scenario generation (Wilby and Dawson 2007). This method has some limitations that are characteristic of statistical downscaling techniques. It is assumed that the future changes in climate can be fully represented by the same

Table 1 Summary of the availability of precipitation data

Station name	Elevation (m msl)	Latitude (°E)	Longitude (°N)	Daily data availability
KTM Airport	1,336	27°42′	85°22′	1970–2005
Daman	2,314	27°63′	85°05′	1970–2005
Sankhu	1,449	27°45′	85°29′	1970–2005
Godavary	1,400	27°34′	85°24′	1970–2005
Khopasi	1,517	27°35′	85°31′	1970–2005
Hariharpurgadhi	250	27°20′	85°30′	1970–2005
Sindhuligadhi	1,463	27°17′	85°58′	1970–2005
Ramolibariya	152	27°01′	85°23′	1970–2005
Pattharkot	275	27°05′	85°40′	1970–2005

Source: DHM, Nepal

set of predictors that are used for the calibration of a predictor–predictand relationship, and this relationship will be valid also under future climatic conditions. In fact, this hypothesis is not verifiable and may not be true (Segui et al. 2009).

3.2.2 Calibration and validation of the downscaling model

The calibration of the SDSM model develops the relation between large-scale screened predictor variables and observed station data (predictand) using the principle of multiple regression. Prior to calibration, the screening of the 26 predictor variables was carried out to select the best set of predictors that produce a good correlation with the predictand (Wilby and Dawson 2007). While screening predictors, it was considered that at least one predictor should significantly correlate with the predictand variable for each of the months. The significance level was taken to be 0.05 %. The correlation matrix developed between a set of predictors and predictands (Table 2) provides the basis for the selection of a set of predictors that are most significantly correlated to the predictand. The scatter plot between predictor and predictand was also used for screening the predictors. The selected predictors based on daily values for maximum and minimum temperatures and precipitation are presented in Table 3.

SDSM provides monthly, seasonal, and annual calibration options. Noticing the monthly variation in the climate of the basin, the monthly calibration option was used for the study. Monthly calibration develops the parameters of downscaling for each month using daily data. Out of the two calibration options available in the model, the unconditional calibration option was used for minimum and maximum temperatures. On the other hand, the conditional option was used for calibrating precipitation, since the precipitation amount depends on intermediate processes like the number of wet/dry days (Wilby et al. 2002). The model also provides a bias correction option. While calibrating the model for precipitation, the bias correction factor was adjusted through trial and error to reduce the bias of simulated precipitation (Khan et al. 2006, Wilby et al. 2002).

The period of 1970–2000 was chosen for model calibration and validation because observed climatic data in the BRB is available from 1970 onwards. Other similar studies have used this period as a base period, since observed data is accessible for many parts of the world during this period (Carter et al. 2007). The calibration and validation of the model was done, respectively, for the 1970–1989 and 1990–2000 periods. The calibrated predictor–predictand relationship based on daily values was used to generate daily climatic data of maximum temperature (T_{max}), minimum temperature (T_{min}), and Precipitation (Prcp). Then, this simulated data was compared with observed station data to validate the model. For validation, mean daily value, standard deviation, and monthly maximum value of each simulated data were compared with corresponding values of observed station data. In case of precipitation, wet-spell and dry-spell lengths were also compared because these events directly affect the regional climate (Dibike and Coulibaly 2005).

3.2.3 Future climate predictions

Calibrated predictor–predictand models were used to generate downscaled climate data for future time periods using the same set of predictor variables as used in the calibration and supplied by HadCM3 GCM under two emission scenarios, A2 and B2. Scenario A2 describes a world with a continuously increasing population with regional orientation in terms of economy and culture, while B2 represents a world in which the emphasis is on local solutions to economic, social, and environmental sustainability with a continuously increasing population (lower than A2) and intermediate economic development (Carter et al. 2007). As A2 and B2 represent the world with two different trends in terms of social, cultural, and economic structures, and both scenarios are analyzed in this study.

Table 2 Correlation matrix developed during the screening of predictor variables for downscaling daily maximum temperature at the KTM Airport station

Analysis period: 1/1/1971–12/31/1989
Significance level: 0.05
Total missing values: 90
Predictand: T_{max} KTM Airport 1971–2000 data

Predictors	Jan	Feb	Mar	Apr	May	Jun	Jul	Aug	Sep	Oct	Nov	Dec
Ncepmslpas.dat	0.009		0.020	0.055	0.033	0.023	0.010			0.046	0.015	0.046
Ncepp_uas.dat	0.010	0.041	0.048	0.028	0.060	0.102	0.064	**0.080**	0.020	**0.171**	**0.171**	0.142
Ncepp500as.dat	**0.442**	**0.226**	**0.279**	0.058	0.157	0.052	**0.276**	0.066	**02091**	0.112	0.167	**0.299**
Nceprhumas.dat	0.053	0.191	0.258	**0.226**	**0.281**	**0.141**	0.035	0.023	0.010		0.013	0.032

The values in bold represent the strongest correlation in each month. The blank spaces symbolize that the predictor/predictand relationship is insignificant for that month as per the selected 0.05 % significance level

Table 3 Predictors used in the study

Predictand	Predictors (NCEP reanalysis)	Partial r
Maximum temperature	Mean sea level pressure (mslp)	−0.567
	Surface zonal velocity (P_u)	−0.318
	500 hpa geopotential height (P^{500})	0.617
	Near-surface relative humidity (rhumas)	−0.265
Minimum temperature	Mean sea level pressure (mslp)	−0.817
	500 hpa geopotential height (P^{500})	0.814
	Relative humidity at 850 hpa (r^{850})	0.512
Precipitation	Mean sea level pressure(mslp)	0.220
	Near surface relative humidity (rhumas)	0.146

For both temperature and precipitation, 20 ensembles were generated for the period of 1961 to 2099. Then, the most reliable ensemble was chosen based on the comparison of the simulated and observed data. Using downscaled results, projected changes in maximum/minimum temperature and precipitation for three time periods: 2010–2039, 2040–2069, and 2070–2099 (addressed as 2020s, 2050s, and 2080s), relative to base period 1970–1999 (1980s), were calculated for all the stations. The average change over the basin was calculated by averaging the results from all the stations.

3.3 Climate change impact on hydrology

3.3.1 Rainfall–runoff modeling

The rainfall–runoff process was simulated using the semidistributed hydrological model Hydrologic Engineering Center's Hydrologic Modeling System (HEC-HMS), version 3.3, developed by the United States Army Corps of Engineers. HEC-HMS is chosen since it provides the user a choice among a number of loss, direct runoff, base flow, and channel routing methods (McColl and Aggett 2007). This is a widely used model in hydrological analyses and it can be used in different climatic and topographical conditions (e.g., Knebl et al. 2005, McColl and Aggett 2007, Markus et al. 2007, Sharma et al. 2007, Chen et al. 2009, Chu and Steinman 2009, Garcı´a et al. 2008). The hydrological model setup with HEC-HMS includes the setting up of (1) a basin model, (2) a meteorological model, and (3) control specification.

Basin geometry such as sub-basin area, slope, longest flow path at each sub-basin, and basin centroid are primary parameters that are used to estimate other basin parameters required for developing a hydrological model with HEC-HMS. The basin model for the study was set up within an HEC-GeoHMS platform. This was done through the process of basin delineation using HEC-GeoHMS version 1.1 that works with ArcView GIS 3.2 (USACE 2003). The basin model developed within HEC-GeoHMS, consisting of sub-basins and their respective areas, stream networks, connectivity of sub-basins, stream reaches, junctions, and outlet points, was imported to the HEC-HMS basin model. The model was run for a long period of time. For this reason, the continuous loss model (deficit and constant loss) was selected. The continuous loss model accounts for moisture losses also during the dry period. The Clark unit hydrograph transformation, constant monthly base flow, and lag routing methods were used to develop the basin model. For more information on basin model development, refer to the HEC-HMS technical reference manual (USACE 2000). The meteorological model was developed with the Thiessen Polygon Weight method.

3.3.2 Calibration and validation of the rainfall–runoff model

The rainfall–runoff model was calibrated and validated by comparing the observed daily flow at the Pandheradoban gauging station with simulated flow. Following Garcia et al. (2008) and Sharma et al. (2006), the model was calibrated for the years 1999–2001 and validated for the year 2002. The developed model was then used to simulate the future water availability in the basin. The input data included: digital elevation model (DEM) from SRTM; soil data obtained from the Department of Soil Conservation and Watershed Management, Nepal, for the year 1995; land use data obtained from the Department of Soil Conservation and Watershed Management, Nepal, for the year 1995; daily precipitation data for the period of 1970–2005 from nine stations in the basin collected from the Department of Hydrology and Meteorology (DHM), Nepal; observed flow at Pandheradobhan gauging station for calibration period (1999–2001); and observed flow at Pandheradobhan gauging station for validation period (2002).

HEC-HMS provides four objective functions for optimization, namely the sum of absolute errors, sum of squared residuals, percent error in peak, and peak weighted root mean square error to adjust the model's parameters (USACE 2000). These options are used for automatic calibration, followed by manual calibration to better identify

and adjust the significant parameters (Garcı´a et al. 2008). Since the major objective of this study is to assess the climate change impact on stream flow and water availability, priority was given to adjust the simulated and observed hydrograph volume. At the same time, the peak and time to peak were also calibrated as far as possible. Three statistical parameters, i.e., R^2, Nash–Sutcliffe efficiency (NSE) coefficient (Nash and Sutcliffe 1970), and relative volume error (VE) were used to quantify the model's performance during calibration and validation.

3.3.3 Scenario runs and impact assessment

Four scenario runs, each of 30-year periods, were developed for both SRES scenarios A2 and B2. The period of 1970–1999 was considered as the baseline period. The changes relative to the baseline period were considered for three future periods 2020s, 2050s, and 2080s. To analyze the climate change impact on streamflow, monthly, seasonal, and annual variations on water availability were calculated for each of the future time period.

To assess spatial variations of climate change impact within the basin, first, the changes in future water availability were calculated for the whole study area and then separate calculations were done for the upper and middle basins. This division of the study area into upper and middle parts was done keeping in mind climatic, physiographical, and social factors within the basin. The upper basin is located mostly in the higher altitudes and has a comparatively colder climate and a higher population density than the middle part. The dominant land use in the upper basin is forestry, cultivation, and built-up area, while most of the area of middle basin is forests, bush, and barren land.

The study assumes no change in the land use/land cover in the upper and middle parts of the BRB for the future periods. Hence, the evaporation/evapotranspiration remains constant and the calibrated and validated model is considered valid for estimating streamflow and water availability in the basin for the future periods.

4 Results and discussion

4.1 GCM climate scenarios

4.1.1 SDSM validation

Validation results of maximum/minimum temperature and precipitation are shown in Figs. 2 and 3, respectively. The graphs show good agreement between the observed and simulated values of mean daily T_{max}, T_{min}, and Prcp for each month. For T_{max}, the maximum difference between the observed and simulated mean values is 1.7 °C (Fig. 2a) in the month of April, and this difference is lower in T_{min}, with a value of 0.8 °C in the same month (Fig. 2d).

The R^2 value for temperature and precipitation significantly increases with downscaled data for both SRES scenarios A2 and B2 (Table 4). Here, statistical calculations have been done with monthly average data. The SD value with downscaled data is more close to the SD of observed data for both scenarios. These statistical results indicate that the downscaling technique has significantly improved the quality of GCM data. Overall, the validation results show that the model can reliably simulate the mean daily precipitation that means that the downscaled data can be used with considerable accuracy to analyze the changes in future water availability.

4.1.2 Future temperature

All the stations in the basin reflect an increasing trend in temperature compared to the baseline period. However, there is spatial variation in the magnitude of the trend. The results show that the highest rise in annual average of T_{max} is predicted in the Kathmandu Airport station with an increase of 2.4 °C by the 2080s, and the lowest increase is predicted in the Daman station with a value of 1.7 ° C by the 2080s for scenario A2. The basin average annual mean of T_{max} is predicted to increase by 2.1 °C under A2 scenario and by 1.5 °C under B2 scenario in 2080s. Table 5 shows the interseasonal variations in increase in T_{max} for the basin. Scenario A2 shows higher increase of T_{max} in spring, while scenario B2 shows higher increase in summer during all three future periods (Table 5).

Monthly future temperature analysis shows the highest rise in March and the lowest rise in January in most of the stations as well as average basin temperature for both scenarios A2 and B2. The analysis results in a monthly basis of future temperature showing the highest warming in March and the lowest warming in January at most of the stations as well as in the whole BRB under both A2 and B2 scenarios.

4.1.3 Future precipitation

Projected precipitation does not show any significant trend for both A2 and B2 scenarios. Similar results were obtained by Shrestha et al. (2000) and PA (2009). There are wide temporal and spatial variations throughout the basin. Scenario A2 shows a decrease of basin average precipitation during winter and spring and increase during the summer (Fig. 4a). On the other hand, scenario B2 shows an increase in precipitation during all the seasons (as seen in Fig. 4b).

To analyze the precipitation anomalies in the basin, percentage change for three future periods, the 2020s, 2050s, and 2080s, relative to the baseline period of 1980s, was calculated with downscaled precipitation under two scenarios for all stations considered in this study. The basin

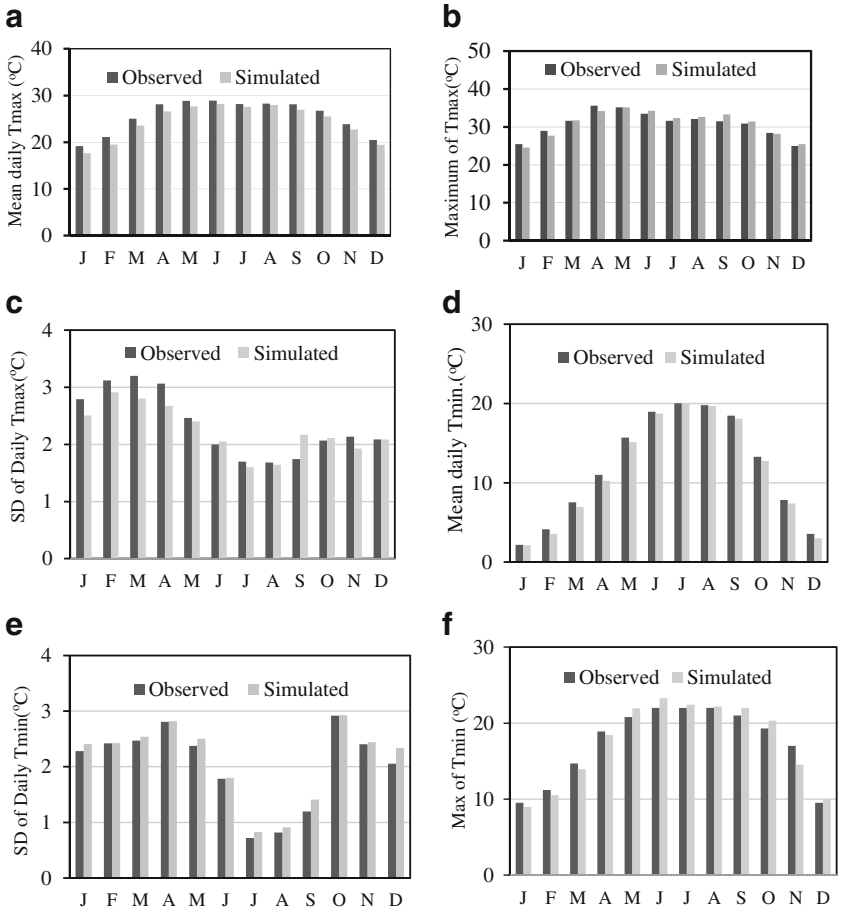

Fig. 2 Comparison of observed and simulated maximum and minimum temperatures during the validation period (1990–2000)

average precipitation was calculated using the Thiessen polygon weights. Scenario A2 shows increases in basin average annual precipitation by 2.0, 7.3, and 13.2 %, respectively, for the 2020s, 2050s, and 2080s (Fig. 4a). Scenario B2 shows increases of 10.4, 14.9, and 17.5 % for the 2020s, 2050s, and 2080s, respectively, which is higher compared to increase predicted under A2 scenario (Fig. 4b).

When studying spatial variation, a mixed trend was observed. For scenario A2, all the stations in the upper basin, except the KTM Airport station, shows decrease in precipitation (Table 6a). On the other hand, all the stations in the middle basin, except Khopasi, show an increase in precipitation in the future. This indicates that for scenario A2, climate change may result in a slight reduction of annual precipitation in the upper basin, while the middle basin may have increased precipitation. However, this increased precipitation is obtained mainly due to a higher increase of precipitation during the monsoon season.

On the contrary, scenario B2 shows an increase in mean annual precipitation all over the basin (Table 6b). However, the rate of increase is higher in the middle than in the upper basin.

4.2 Calibration and validation of the HEC-HMS model

4.2.1 Observed precipitation

The comparison of observed and simulated flows at Pandheradoban for calibration (Fig. 5a) and validation (Fig. 5b) periods shows a good agreement. The time to peak and number of peak were represented well by simulated flow. However, the model could not follow the magnitude of the peak well. Previous studies with HEC-HMS modeling for daily data also came up with similar results (e.g., Garcı´a et al. 2008).

During calibration, R^2 and NSE values of 0.71 and 0.69, respectively, were obtained, indicating a good agreement between observed and simulated flows. During validation, both R^2 and NSE values were found to be 0.66, which is within the considerable range. The NSE value between 0.5 and 0.95 indicates good simulation results (Andersen et al. 2001). The model's hydrograph volume almost matches the observed hydrograph volume during both calibration and validation. The model overpredicts the hydrograph volume during calibration by 1.2 %, while it underpredicts it during validation by 5.78 %. The model results with VE of less than 10 % are considered satisfactory and below 5 % are

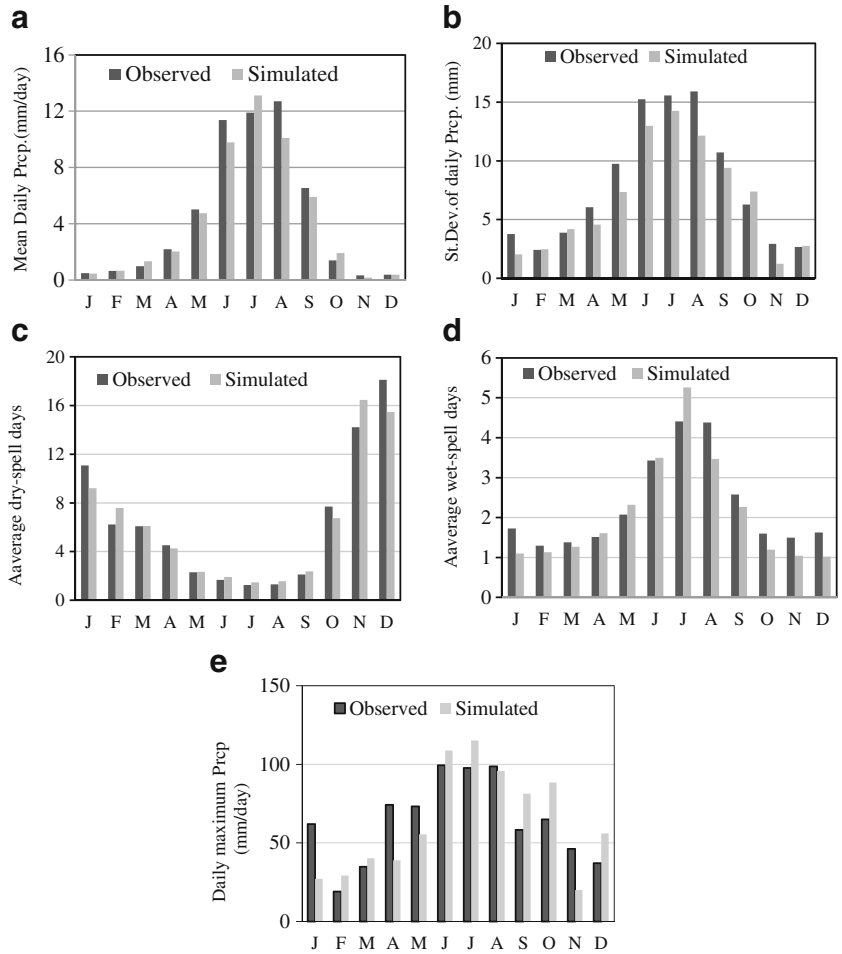

Fig. 3 Comparison of observed and simulated precipitation during the validation period (1990–2000)

considered excellent (Xu et al. 2008). This minor error in simulating the volume of the hydrograph indicates that the model is capable of simulating the volume of water available during present and future time periods. The statistical results of model calibration and validation indicate that the model can be used with calibrated basin parameters to simulate flow for a future time period. From calibration, it was found that the storage coefficient, the initial deficit, and the constant loss parameters are most significant when adjusting the hydrograph's volume and peak flow, while time of concentration, lag time, and storage coefficient determine time to peak.

4.2.2 Downscaled precipitation

To check the performance of downscaled rainfall to simulate river flow for a future time period, the calibrated model was run with downscaled rainfall for scenarios A2 and B2 for the time period 1999–2001 and then monthly average flow obtained from each of the runs was compared with the monthly average observed flow for the same period. The analysis of downscaled precipitation to simulate the flow for period 1999–2001 shows that scenarios A2 and B2 have volume biases of −2.6 and 2 %, respectively (Table 7). The R^2 of monthly average flows for downscaled scenarios A2 and B2 with observed monthly flow

Table 4 Summary statistics of raw and downscaled GCM data at Kathmandu Airport station for period 1990–2000

		Observed	A2		B2	
			GCM raw	Downscaled	GCM raw	Downscaled
Max. temperature	SD (°C)	3.63	5.46	3.67	5.58	3.91
	R^2	–	0.61	0.89	0.54	0.87
Min. temperature	SD (°C)	2.7	4.9	2.7	5.1	2.9
	R^2	–	0.7	0.99	0.56	0.94
Precipitation	SD (mm)	4.89	14.17	4.6	2.91	4.63
	R^2	–	0.4	0.87	0.52	0.81

The statistics is presented here for monthly average values of T_{max}, T_{min}, and Prcp

Table 5 The basin average change in seasonal T_{max} for three future time periods relative to the baseline period (1980s)

	Winter		Spring		Summer		Autumn		Annual	
Scenario → / Period ↓	A2	B2	A2	B2	A2	B2	A2	B2	A2	B2
2020s	0.4	0.4	0.7	0.5	0.5	0.5	0.5	0.5	0.5	0.5
2050s	1.0	0.9	1.2	0.9	1.2	1.1	1.0	0.8	1.1	0.9
2080s	1.8	1.4	2.4	1.6	2.1	1.7	1.9	1.3	2.1	1.5

are 0.96 and 0.93, respectively. All these statistical analyses imply that downscaled precipitation can simulate the monthly average flow hydrograph and water availability with considerable accuracy.

4.3 Impact on streamflow and water resources

4.3.1 Streamflow

The impact on streamflow and water resources was analyzed for wet season and dry season. The wet season (June to September) is the same as the summer season as considered in this study, and dry season (October to May) comprises winter, spring, and autumn. To further represent the results, dry season is divided into two parts, premonsoon (Jan–May) and postmonsoon (Oct–Dec).

The plot of monthly average flow for the baseline period and three future periods shows that the hydrograph ordinates for future time periods diminish during premonsoon months (Jan–May), except April, while they significantly increase during the monsoon (Jun–Sep) and postmonsoon (Oct–Dec) periods. The monthly average peak shifts to August in the 2080s, while it is obtained in July for the baseline period, 2020s, and 2050s (Fig. 6a). Hydrograph ordinates decrease during premonsoon and increase during postmonsoon; the shifting of the peak from July to August clearly indicates slight changes in seasonal water availability. Scenario A2 predicts a very significant increase in the average monthly flow during the monsoon period and the month of August has the highest increase with 28.6 % increase in 2080. As seen in Fig. 6b, scenario B2 indicates an increase in hydrograph ordinates during most of the time of the year, except March, and the peak of the hydrograph occurs in July for all future time periods. This scenario also predicts the slight widening of the monsoon hydrograph with an increase in pre- and postmonsoon ordinates.

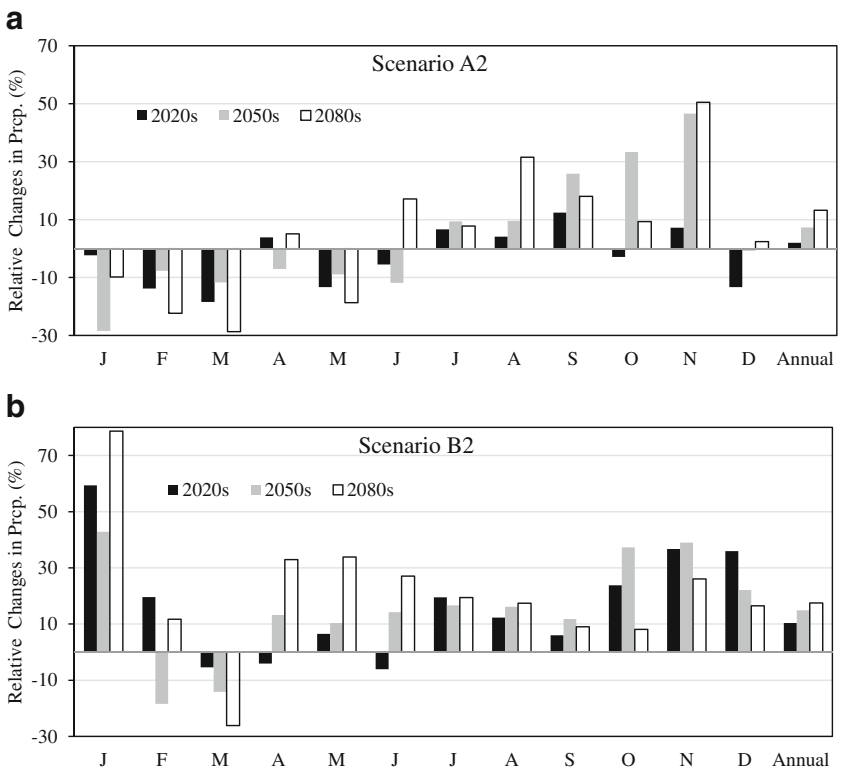

Fig. 4 Changes in basin average monthly precipitation for three future periods relative to the baseline period (1980s). **a** Scenario A2 and **b** scenario B2

Table 6 Changes in mean annual precipitation (%) in three future periods relative to the baseline period (1980s) in Bagmati River Basin

	Upper basin			Middle basin				
Period	KTM Airport	Daman	Sankhu	Godavary	Khopasi	Sindhuli Gadhi	Hariharpur Gadhi	Ramoli Bariya
Scenario A2								
2020s	7.2	−0.5	−10.3	0.5	−0.9	0.6	7.2	−2.2
2050s	4.0	−2.1	−9.3	−2.6	0.2	8.2	20.1	7.2
2080s	6.4	5.0	−9.8	2.7	−4.0	24.2	29.1	36.3
Scenario B2								
2020s	5.7	0.7	8.1	4.8	2.4	11.8	19.6	9.1
2050s	11.6	9.8	9.9	8.1	10.5	26.5	19.4	6.1
2080s	8.2	2.6	5.9	6.9	4.0	35.3	28.3	20.4

For station location, refer to Fig. 1

4.3.2 Water resources

When analyzing seasonal water variation for the entire BRB, scenario A2 shows a decrease in premonsoon (Jan–May) water availability and an increase in monsoon (Jun–Sep) and postmonsoon (Oct–Dec) water availability in the future. Premonsoon water availability is predicted to decrease by 7.78, 7.23, and 11.35 %, respectively, for the 2020s, 2050s, and 2080s, while for the same time period, the monsoon season's water availability is predicted to increase by 3.28, 5.3, and 16.36 % (Table 8a). This implies that according to scenario A2, the premonsoon season is expected to become drier, and the monsoon and postmonsoon seasons may become wetter. Monthly results represent that all premonsoon months (Jan–May), except April, are expected to experience decrease in water availability, thereby worsening the water stress situation in the basin (Fig. 7a). The monsoon season's months from July to

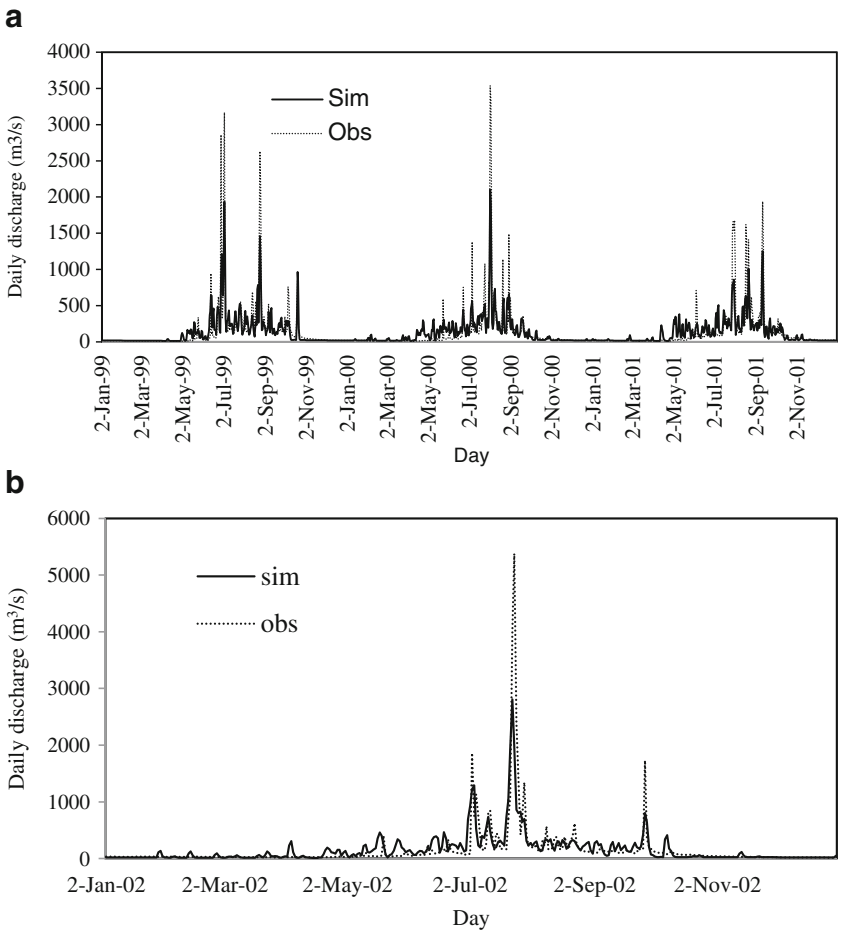

Fig. 5 **a** Comparison of observed and simulated flows at the Pandheradoban gauging station for the calibration period (1 Jan 1999 to 31 Dec 2001). **b** Comparison of observed and simulated flows at the Pandheradoban gauging station for the validation period (1 Jan to 31 Dec 2002)

Table 7 Performance of downscaled precipitation to simulate monthly average flow and water availability

Model simulation scenarios	Model run with Scenario A2 (1999–2001)	Model run with Scenario B2 (1999–2001)
R^2	0.96	0.93
Volume bias (MCM)	−104.5	79.2
% bias	−2.6	2.0

September and postmonsoon months from October to December may experience an increase in water availability (Fig. 7a). The change in monthly water availability is predicted to vary from 21.54 % decrease in May to 28.64 % increase in August during 2080s. Scenario B2 shows an increase in water availability during both dry and wet seasons (Table 9a). On a monthly scale, scenario B2 shows an increase in water availability in all months, except February and March, as reflected in Fig. 7b during all three future periods. However, there is a wide variation in magnitude.

4.3.3 Spatial variation in future water availability

To assess the spatial variation of climate change impact on future water availability within the basin, the impact study was also conducted separately in the upper and middle basins (Fig. 1). Results show very negligible changes in annual average water availability in the upper basin, i.e., a 0.28 % increase by the 2080s for scenario A2. On the other hand, the middle basin is expected to experience a noticeable 15.61 % increase.

On the seasonal scale, there is a noticeable difference between the upper and middle basins. Scenario A2 shows a decrease in premonsoon water availability, both in the upper and middle basins. However, the decrease in the upper basin (i.e., 16.94 % for the 2080s) is almost double of the middle basin (8.48 % for the 2080s) (Table 8). Results show an increase in the water availability during monsoon, both in the upper and middle basins, but the predicted rate of increase is very low in the upper basin (1.67, 1.3 and 6.61 %, respectively, during the 2020s, 2050s, and 2080s). In the middle basin, increases of 3.90, 6.89, and 20.73 %, respectively, are predicted during

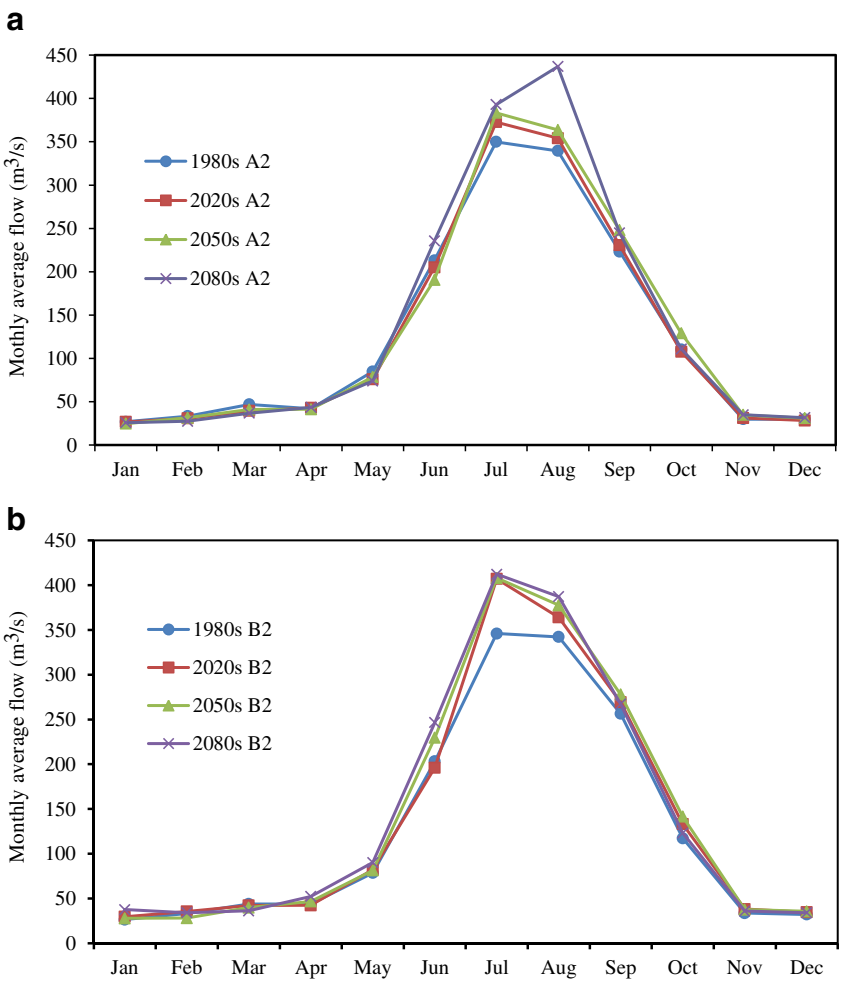

Fig. 6 Monthly average flow hydrographs for the baseline period and three future periods at the Pandheradoban gauging station. **a** Scenario A2 and **b** scenario B2

Table 8 Changes in water availability during three future periods relative to the baseline period (1980s) under scenario A2

Season[a]		Water available during base period (mm)	Future changes in water availability					
			2020s		2050s		2080s	
			mm	%	mm	%	mm	%
(a) Whole basin								
Wet	Monsoon	1,010	33	3.26	54	5.30	165	16.36
Dry	Premonsoon	210	−16	−7.78	−15	−7.23	−24	−11.35
	Postmonsoon	145	−2	−1.53	21	14.73	7	4.59
	Annual	1,365	14	1.04	60	4.43	148	10.82
(b) Upper basin								
Wet	Monsoon	929	16	1.67	12	1.3	61	6.61
Dry	Premonsoon	229	−20	−8.85	−23	−9.88	−39	−16.94
	Postmonsoon	152	−5	−3.14	−2	−1.34	−19	−12.47
	Annual	1,311	−10	−0.73	−13	−0.96	4	0.28
(c) Middle basin								
Wet	Monsoon	1,051	41	3.9	72	6.89	218	20.73
Dry	Premonsoon	202	−15	−7.24	−12	−5.88	−17	−8.48
	Postmonsoon	153	−1	−0.81	34	21.93	19	12.23
	Annual	1,406	25	1.79	94	6.7	219	15.61

[a] Monsoon: Jun–Sep, premonsoon: Jan–May, postmonsoon: Oct–Dec

2020s, 2050s, and 2080s (Table 8b and c). For the postmonsoon season, the upper and middle basins show very different natures of climate change impact for future water availability. The upper part is expected to experience decreases in postmonsoon water availability by 3.14, 1.34, and 12.47 %, respectively, during the 2020s, 2050s, and 2080s, while the middle basin is expected to experience noticeable increases of 21.93 and 12.23 %, respectively, during 2050s and 2080s. During 2020s, the middle basin is expected to experience a decrease of postmonsoon water availability by 0.81 %.

Scenario B2 also predicted spatial variation in water availability during future periods. This scenario predicted less increase in annual average water availability in the upper basin (2.36, 4.77, and 1.87 %, respectively, during the 2020s, 2050s, and 2080s), while it predicted a noticeable increase in the middle basin (9.53, 13.72, and 17.08 %, respectively, for the 2020s, 2050s, and 2080s) as presented in Table 9b and c. On the seasonal scale also, the upper and middle basins show a significant difference in water availability during future periods.

For the entire BRB, the total annual average water availability is predicted to increase by 10.28 % during 2080s for scenario A2. In the upper basin, predicted change is negligible in annual average water availability, but in the middle basin, a noticeable increase is predicted during 2080s. Scenario B2 also predicted less increase in annual average water availability in the upper basin, as compared to the middle basin. This analysis clearly indicates that the climate change impact on water resources varies largely on both the temporal and spatial scales. Therefore, the impact study should be conducted at a finer spatial scale to obtain more precise results. However, the size of the study area can be selected based on the purpose of the study and accuracy required.

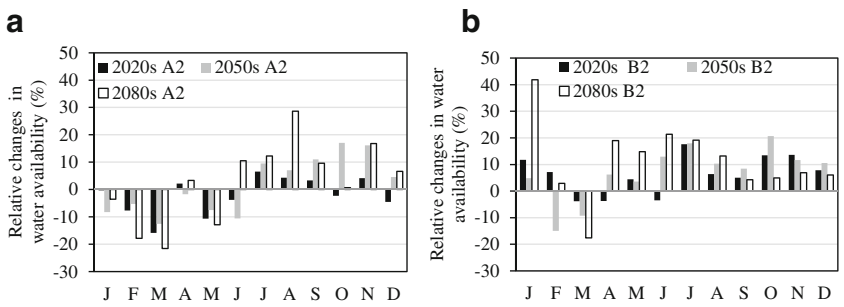

Fig. 7 Percentage changes in monthly water availability during three future periods relative to the baseline period (1980s) for the whole Bagmati River Basin under **a** scenario A2 and **b** scenario B2

Table 9 Changes in water availability in three future periods relative to the baseline period (1980s) under scenario B2

Season[a]		Water available during base period (mm)	Future changes in water availability					
			2020s		2050s		2080s	
			mm	%	mm	%	mm	%
(a) Whole basin								
Wet	Monsoon	1,067	65	6.05	135	12.67	154	14.42
Dry	Premonsoon	210	5	2.50	−2	−0.98	23	10.73
	Postmonsoon	170	21	12.50	29	17.23	9	5.5
	Annual	1,447	91	6.29	162	11.22	186	12.84
(b) Upper basin								
Wet	Monsoon	885	30	3.44	66	7.5	40	4.49
Dry	Premonsoon	218	−4	−1.79	−10	−4.72	2	1.06
	Postmonsoon	154	3	2.03	4	2.48	−18	−11.98
	Annual	1,257	30	2.36	60	4.77	24	1.87
(c) Middle basin								
Wet	Monsoon	1,100	102	9.28	160	14.54	198	18.03
Dry	Premonsoon	197	9	4.63	2	0.88	31	15.55
	Postmonsoon	169	28	16.8	39	23.3	22	12.69
	Annual	1,466	140	9.53	201	13.72	250	17.08

[a] Monsoon: Jun–Sep, premonsoon: Jan–May, postmonsoon: Oct–Dec

5 Conclusions

This paper quantifies the changes in future climate and its impact on the hydrology of the Bagmati River Basin in Nepal. The Hadley Centre Coupled Model, version 3 (HadCM3) GCM was used to capture future temperature and precipitation. The resolution of the HadCM3 is very coarse for hydrological analysis at the basin level. Therefore, a statistical downscaling model (SDSM) was employed to simulate future climate at the station level using large-scale GCM predictors. Downscaling results indicate that the SDSM model was able to estimate both mean and extreme values of temperature and mean values of precipitation with considerable reliability. Results show a higher rise in temperature during summer as compared to winter. Future average annual basin precipitation is predicted to increase under both A2 and B2 scenarios. However, dry season is expected to become drier and wet season is expected to become wetter under the A2 scenario.

The HEC-HMS model was used to analyze the hydrological impact of climate change in terms of streamflow. The 30-year period of 1970–1999 was considered as the baseline period and was used in comparison with three future periods: 2010–2039 (2020s), 2040–2069 (2050s), and 2070–2099 (2080s) for impact analysis. It is anticipated that the annual water availability during all three future periods may increase under both A2 and B2 scenarios, indicating that the basin as a whole become wetter when water accounting is done annually. The increase in annual water availability towards the end of the century may vary between 10.82 and 12.84 %. There may also be a wide variation in seasonal and monthly water availability. Under A2 scenario, the premonsoon water availability may decrease, indicating a worsening situation of water stress during the dry season. However, an increase in the postmonsoon water availability may relieve the water stress situation to some extent. In contrast, under B2 scenario, water availability is expected to increase during both wet and dry seasons. Higher water availability during the wet season under both A2 and B2 scenarios may worsen the flood situation in the future.

To assess the spatial variation of climate change impact on water availability within the basin, a separate analysis was done for the upper and middle basins. Under A2 scenario, annual average water availability in future periods is expected to register negligible changes in the upper basin, while the middle basin may witness a noticeable increase. During the dry season, premonsoon water availability is predicted to decrease in both the upper and middle basins with higher rate of decrease in the upper basin, whereas the postmonsoon water availability is predicted to decrease in the upper basin and increase in the middle basin. Increase in water availability is predicted during wet season for both parts of the basin with a higher rate of increase for the middle basin. Under B2 scenario, both parts of the basin are predicted to have a noticeable increase in annual water

availability, but the increase is expected to be comparatively higher in the upper basin. The broad range of hydrologic predictions from this study is expected to help decision-making for sustainable water management in the Bagmati River Basin become more informed and efficient.

As noted earlier, this study has not considered the changes in land use/land cover as well as water demands due to socioeconomic development in the future. A comprehensive research considering the uncertainties in future climate affecting the water availability as well as predicting the future land use/land cover and demands for water by various economic sectors including ecological demand is suggested.

Acknowledgments The authors are grateful to officials of the Department of Hydrology and Meteorology, Nepal, for their cooperation during the data collection and the Church of Scotland, UK, for providing research funds.

References

Andersen J, Refsgaard JC, Jensen HK (2001) Distributed hydrological modeling of the Senegal River Basin-model construction and validation. J Hydrol 247:200–214

Arnell NW (2003) Effect of IPCC SRES emissions scenarios on river runoff: a global perspective. Hydrol Earth Syst Sci 7(5):619–641

Arora VK, Boer GJ (2001) Effects of simulated climate change on the hydrology of major river basins. J Geophys Res 106:3335–3348

Babel MS, Pandey VP, Rivas AA, Wahid SM (2011) Indicator-based approach for assessing the vulnerability of freshwater resources in the Bagmati River basin, Nepal. Environ Manag 48(5):1044–1059

Carter TR, Alfsen K, Barrow E, Bass B, Dai X, Desanker P et al. (2007) IPCC-TGICA: general guidelines on the use of scenario data for climate impact and adaptation assessment (TGICA), version 2

Chen Y, Xu Y, Yin Y (2009) Impacts of land use change scenarios on storm-runoff generation in Xitiaoxi basin, China. Quat Int xxx:1–8

Chiew FHS, Teng J, Vaze J, Kirono DGC (2009) Influence of global climate model selection on runoff impact assessment. J Hydrol 379:172–180

Christensen N, Wood WA, Voison N, Lettenmaier DP (2004) The effects of climate change on the hydrology and water resources of the Colorado River Basin. Clim Chang 62:337–363

Chu X and Steinman A (2009) Event and continuous hydrologic modeling with HEC-HMS. J. Irrig. Drain Eng January/February 119

Dibike YB, Coulibaly P (2005) Hydrologic impact of climate change in the Saguenay watershed: comparison of downscaling methods and hydrologic models. J Hydrol 307:145–163

Dore MHI (2005) Climate change and changes in global precipitation patterns: what do we know? Environ Int 31:1167–1181

Garcı´a A, Sainz A, Revilla JA, A´lvarez C, Juanes JA, Puente A (2008) Surface water resources assessment in scarcely gauged basins in the north of Spain. J Hydrol 356:312–326

Harmsen EW, Miller NL, Schlegel NJ, Gonjalez JE (2009) Seasonal climate change impacts on evapotranspiration, precipitation deficit and crop yield in Puerto Rico. Agric Water Manag 96:1085–1095

Harpham C, Wilby RL (2005) Multi-site downscaling of heavy daily precipitation occurrence and amounts. J Hydrol 312:235–255

Hitz S, Smith J (2004) Estimating global impacts from climate change. Glob Environ Change 14:201–218

Huntingford G, Gash J, Giacomello AM (2006) Climate change and hydrology: next steps for climate models. Hydrol Process 20:2085–2087

IPCC (2001) Climate Change 2001In: Houghton JT, Ding Y, Griggs Dj, Noguer M, Van der Linden PJ, Xiaosu D (2001) The scientific basis contribution of working group 1 to the third assessment report of the IPCC. Cambridge University Press, Cambridge

ISET-N (2009) Vulnerability through the eyes of vulnerable: climate change induced uncertainties and Nepal's development predicaments. Institute for Social and Environmental Transition—Nepal (ISET-N). Kathmandu: Nepal Climate Vulnerability Study Team

Jain SK (2008) Impact of retreat of Gangotri glacier on the flow of Ganga River. Curr Sci 95(8):1012–1014

Khan MS, Coulibaly P, Dibike Y (2006) Uncertainty analysis of statistical downscaling methods. J Hydrol 319:357–382

Knebl MR, Yang ZL, Hutchison K, Maidment DR (2005) Regional scale flood modeling using NEXRAD rainfall, GIS, and HEC-HMS/RAS: a case study for the San Antonio River Basin Summer 2002 storm event. J Environ Manage 75:325–336

Markus M, Angel JR, Yang L, Hejazi MI (2007) Changing estimates of design precipitation in Northeastern Illinois: comparison between different sources and sensitivity analysis. J Hydrol 347:211–222

McColl C, Aggett G (2007) Land-use forecasting and hydrologic model integration for improved land-use decision support. J Environ Manage 84:494–512

Minville M, Brissette F, Leconte R (2008) Uncertainty of the impact of climate change on the hydrology of a Nordic watershed. J Hydrol 358:70–83

Nash JE, Sutcliffe JV (1970) River flow forecasting through conceptual models. Part 1. A discussion of principles. J Hydrol 10:282–290

Nohara D, Kitoh A, Hosaka M, Oki T (2006) Impact of climate change on river runoff. J Hydrometeorol 7:1076–1089

NTNC (2009) Bagmati Action Plan (2009–2014) Government of Nepal & National Trust for Nature Conservation. Kathmandu, Nepal

OECD (2003) Development and climate change in Nepal: focus on water resources and hydropower. Organisation for Economic Co-operation and Development. Available at: http://www.oecd.org/environment/cc/19742202.pdf Retrieved on 11th February, 2013

PA (2009) Temporal and spatial variability of climate change over Nepal (1976–2005). Practical Action, Katmandu

Prudhomme C, Reynard N, Crooks S (2002) Downscaling of global climate models for flood frequency analysis: where are we now? Hydrol Process 16:1137–1150

Rees HG, Holmes MGR, Young AR, Kansakar SR (2004) Recession-based hydrological models for estimating low flows in ungauged catchments in the Himalayas. Hydrol Earth Syst Sci 8(5):891–902

Segui PQ, Ribes A, Martin E, Habets F, Bo J (2009) Comparison of three downscaling methods in simulating the impact of climate change on the hydrology of Mediterranean basins. J Hydrol. doi:10.1016/j.jhydrol.2009.09.050

Sharma D, Gupta AD, Babel MS (2007) Spatial disaggregation of bias-corrected GCM precipitation for improved hydrologic simulation: Ping River Basin, Thailand. Hydrol Earth Syst Sci 4:35–74

Shrestha AB, Wake CP, Mayewski PA, Dibb JE (1999) Maximum temperature trends in the Himalaya and its vicinity: an analysis based on temperature records from Nepal for the period 1971–94. Am Meteorol Soc 12:2775–2786

Shrestha AB, Wake CP, Dibb JE, Mayewski PA (2000) Precipitation fluctuations in the Nepal Himalaya and its vicinity and

relationship with some large scale climatologically parameters. Int J Climatol 20:317–327

Sharma RJ, Shakya NM (2006) Hydrological changes and its impact on water resources of Bagmati watershed, Nepal. J Hydrol 327:315–332

Toews MW, Allen DM (2009) Evaluating different GCMs for predicting spatial recharge in an irrigated arid region. J Hydrol 374:265–281

USACE (2000) Hydrologic modeling system HEC-HMS: technical reference manual. US Army Corps of Engineers, Hydrologic Engineering Center, Davis

USACE (2003) Geospatial hydrologic modeling extension, HEC-GeoHMS: user's manual, version 1.1. US Army Corps of Engineers, Hydrologic Engineering Center, Davis

WECS (2011) Water resources of Nepal in the context of climate change, Water and Energy Commission Secretariat (WECS)

Wilby RL and Dawson CW (2007) SDSM 4.2—a decision support tool for the assessment of regional climate change impacts, user manual

Wilby RL and Dawson CW (2004) Using SDSM version 3.1—a decision support tool for the assessment of regional climate change impacts. Nottingham, UK

Wilby RL, Dawson CW, Barrow EM (2002) SDSM—a decision support tool for the assessment of regional climate change impacts. Environ Model Softw 17(2):147–159

Wilby RL, Whitehead PG, Butterfield D, Wade AJ, Davis RJ, Watts G (2006) Integrated modeling of climate change impacts on water resources and quality in a lowland catchment: River Kennet, UK. J Hydrol 330:204–222

Xu ZX, Zhao FF, Li JY (2008) Response of stream flow to climate change in the headwater catchment of the Yellow River basin. Quat Int XXX:1–14